Int. J. Solids Structures, 1969, Vol. 5, pp. 795 to 816. Pergamon Press. Printed in Great Britain

INDENTATIONS OF AN ELASTIC LAYER BY MOVING PUNCHES

C. SVE†
Aerospace Corporation, El Segundo, California

and

L. M. KEER‡
The Technological Institute, Northwestern University, Evanston, Illinois

Abstract—A layer in plane strain (or stress) is indented by two frictionless punches of a given profile moving at a uniform velocity along its surfaces. Symmetry about the midsurface of the layer is preserved and Fourier transforms are utilized to reduce the problem to the solution of a set of dual integral equations. Standard techniques yield a Fredholm integral equation that is solved numerically for parabolic and wedge punches. Results for the static case are compared with a photoelastic experiment. An analysis including the effects of prestress is briefly presented.

INTRODUCTION

THE problems to be considered here involve the steady motion of frictionless indenters on an elastic layer, and all solutions will be appropriate to plane elasticity. Literature on the general theory and related problems is extensive. E. Yoffe [1] has investigated the problem of steady motion of a Griffith crack in an elastic material utilizing the method of Fourier transforms. Sneddon [2] has formulated related dynamic plane elasticity problems involving steady motion by using a stress function approach involving functions of complex variables. Radok [3] has applied the same method independently to solve several problems including that of a parabolic punch moving on a half-plane. The stress functions that arise from these analyses are solutions to a biharmonic type of equation.

Sneddon and Berry [4] discuss the two approaches to dynamic elasticity problems, i.e. the complex variable method and the integral transform method. The problem of a moving pressure pulse on a half-plane and the problem of a moving dislocation are included as examples for the complex variable method. A variable pressure applied to a half-plane is considered using integral transform techniques. All motions are with velocities below the Rayleigh speed. Cole and Huth [5] have considered the problem of a line load moving at a steady velocity over a half-plane, where all velocity ranges are considered. Ang [6] discusses the Rayleigh resonance phenomena by solving the transient problem for the line load moving with a velocity varying as a step function of time. Payton [7] solves the transient problem of a suddenly applied line load which then moves with a constant velocity for all ranges of velocity.

Elastic plate problems have also attracted interest since their solutions have many practical applications. Fourier integral transform techniques were utilized by Morley [8] to obtain the steady motion solution for an elastic plate with loads traveling along its surfaces.

† Member of the Technical Staff; formerly Graduate Student, Department of Civil Engineering, The Technological Institute, Northwestern University, Evanston, Illinois.
‡ Associate Professor of Civil Engineering.

Problems involving semi-infinite solids to which moving pressures are applied have been considered by Eason [9] and Payton [10]. Eason considers the three-dimensional steady motion of a pressure distributed over a circular or rectangular area on the surface of the half-space. Payton has investigated the half-space problem for suddenly applied point force, which then moves with uniform velocity.

Problems involving prestress have been treated by many authors. Books by Biot [11] and Green and Adkins [12] summarize elasticity theories that include large initial stresses. Wright [13, 14] has solved certain problems related to the present work based upon theories developed by Green, Rivlin and Shield [15] and Novozhilov [16] indicating that several different approaches to the initial stress problem are available. For steady-state dynamic problems, the equations of equilibrium are similar to those obtained for anisotropic elasticity and may be treated as in Green and Zerna [17]. Chen [18, 19] has exploited this approach for transversely isotropic materials. In a prestressed material the critical speeds change from that of the unstressed state. Buckens [20] has studied the velocity of Rayleigh waves in a prestressed semi-infinite medium over a wide range of parameters.

The particular problems to be studied here involve the steady motion of rigid indenters on an elastic strip. Separately considered are the cases of isolated indenters moving on an unstressed or prestressed strip.

ANALYSIS

Symmetric case

Stress distributions in an isotropic elastic layer are studied. A fixed coordinate system (x', y', z') is defined as shown in Fig. 1. The equations of two-dimensional elasticity in terms of these coordinates are used to formulate the problem [8], and the equations of equilibrium are given by

$$\frac{\partial \sigma_x}{\partial x'}+\frac{\partial \tau_{xy}}{\partial y'}=\rho\frac{\partial^2 u}{\partial t^2}, \qquad \frac{\partial \tau_{xy}}{\partial x'}+\frac{\partial \sigma_y}{\partial y'}=\rho\frac{\partial^2 v}{\partial t^2}, \tag{1}$$

where σ_x, σ_y, and τ_{xy}, are the stress components, t is time, ρ is the mass density, and u, v are the displacements in the x', y' directions, respectively. The assumption of small displacements and application of Hooke's law yield the following stress displacement equations:

$$\sigma_x=\lambda\left(\frac{\partial u}{\partial x'}+\frac{\partial v}{\partial y'}\right)+2\mu\frac{\partial u}{\partial x'}, \qquad \sigma_y=\lambda\left(\frac{\partial u}{\partial x'}+\frac{\partial v}{\partial y'}\right)+2\mu\frac{\partial v}{\partial y'},$$
$$\tau_{xy}=\mu\left(\frac{\partial u}{\partial y'}+\frac{\partial v}{\partial x'}\right), \tag{2}$$

where λ and μ are Lamé's constants and the plate is in plane strain.

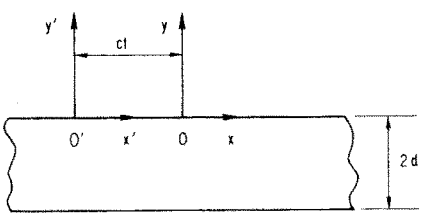

FIG. 1. Coordinate geometry.

To solve the governing set of equations, two potentials, Φ and Ψ, are introduced with the displacements given by

$$u = \frac{\partial \Phi}{\partial x'} + \frac{\partial \Psi}{\partial y'}, \qquad v = \frac{\partial \Phi}{\partial y'} - \frac{\partial \Psi}{\partial x'}, \tag{3}$$

where Φ, Ψ are functions of x', y' and t. Substituting equation (3) into (1) and (2) leads to

$$\sigma_x = \lambda \nabla^2 \Phi + 2\mu \left(\frac{\partial^2 \Phi}{\partial x'^2} + \frac{\partial^2 \Psi}{\partial x' \partial y'} \right), \qquad \sigma_y = \lambda \nabla^2 \Phi + 2\mu \left(\frac{\partial^2 \Phi}{\partial y'^2} - \frac{\partial^2 \Psi}{\partial x' \partial y'} \right),$$
$$\tau_{xy} = \mu \left(2 \frac{\partial^2 \Phi}{\partial x' \partial y'} - \frac{\partial^2 \Psi}{\partial x'^2} + \frac{\partial^2 \Psi}{\partial y'^2} \right). \tag{4}$$

The equations of motion (1) reduce to the two wave equations

$$c_1^2 \nabla^2 \Phi = \partial^2 \Phi / \partial t^2, \qquad c_2^2 \nabla^2 \Psi = \partial^2 \Psi / \partial t^2, \tag{5}$$

where

$$c_1^2 = (\lambda + 2\mu)/\rho, \qquad c_2^2 = \mu/\rho, \qquad \nabla^2 = \frac{\partial^2}{\partial x'^2} + \frac{\partial^2}{\partial y'^2}. \tag{6}$$

Rigid indenters are assumed to be moving with constant velocity c along the layer surfaces in the x' direction. Using the moving coordinate system x, y, z defined as

$$x = x' - ct, \qquad y = y', \qquad z = z', \tag{7}$$

the variable time is eliminated from the analysis. The wave equations become

$$\beta_1^2 \frac{\partial^2 \Phi}{\partial x^2} + \frac{\partial^2 \Phi}{\partial y^2} = 0, \qquad \beta_2^2 \frac{\partial^2 \Psi}{\partial x^2} + \frac{\partial^2 \Psi}{\partial y^2} = 0, \tag{8}$$

where

$$\beta_1^2 = 1 - \frac{c^2}{c_1^2}, \qquad \beta_2^2 = 1 - \frac{c^2}{c_2^2}. \tag{9}$$

Considering an indentation symmetrical with respect to the y axis, the Fourier transforms [21]

$$\bar{\Phi}(\xi, y) = \int_0^\infty \Phi(x, y) \cos(\xi x)\, dx, \qquad \bar{\Psi}(\xi, y) = \int_0^\infty \Psi(x, y) \sin(\xi x)\, dx, \tag{10}$$

are introduced, whose inverses are

$$\Phi(x, y) = \frac{2}{\pi} \int_0^\infty \bar{\Phi}(\xi, y) \cos(\xi x)\, d\xi, \qquad \Psi(x, y) = \frac{2}{\pi} \int_0^\infty \bar{\Psi}(\xi, y) \sin(\xi x)\, d\xi.$$

The boundary conditions for the problem to be studied are

$$\begin{aligned} \sigma_y &= 0, & y &= 0, & |x| &> l, \\ \tau_{xy} &= 0, & y &= 0, & -\infty &< x < \infty, \\ v &= w(x), & y &= 0, & |x| &< l, \\ \tau_{xy} &= v = 0, & y &= -d, & -\infty &< x < \infty, \end{aligned} \tag{11}$$

where $w(x)$ is an even function of x, $2l$ is the punch width, and $2d$ is the layer thickness. The boundary conditions imply symmetry about the plane $y = -d$. The solution to the governing equations is decomposed into a half-plane solution and an undamaged layer solution, which is

$$\Phi(x, y) = \Phi_h(x, y) + \frac{2}{\pi}\int_0^\infty [A_1(\xi)\mathrm{ch}(\xi\beta_1 y) + B_1(\xi)\mathrm{sh}(\xi\beta_1 y)]\xi^{-2}\cos(\xi x)\,\mathrm{d}\xi,$$
$$\Psi(x, y) = \Psi_h(x, y) + \frac{2}{\pi}\int_0^\infty [A_2(\xi)\mathrm{ch}(\xi\beta_2 y) + B_2(\xi)\mathrm{sh}(\xi\beta_2 y)]\xi^{-2}\sin(\xi x)\,\mathrm{d}\xi, \tag{12}$$

where

$$\Phi_h(x, y) = -\frac{2(1+\beta_2^2)}{\pi\mu R}\int_0^\infty \xi^{-2}\gamma(\xi)\,\mathrm{e}^{\xi\beta_1 y}\cos(\xi x)\,\mathrm{d}\xi,$$
$$\Psi_h(x, y) = -\frac{4\beta_1}{\pi\mu R}\int_0^\infty \xi^{-2}\gamma(\xi)\,\mathrm{e}^{\xi\beta_2 y}\sin(\xi x)\,\mathrm{d}\xi, \tag{13}$$

and

$$R = (1+\beta_2^2)^2 - 4\beta_1\beta_2. \tag{14}$$

This solution must satisfy boundary conditions (11). The stress boundary conditions on $y = 0$ lead to

$$B_1 = \frac{A}{2\beta_1}, \qquad A_2 = \frac{A}{1+\beta_2^2}, \qquad A_1 = \frac{B}{1+\beta_2^2}, \qquad B_2 = \frac{B}{2\beta_2}, \tag{15}$$

where A and B are functions of ξ. The boundary conditions on $y = -d$ lead to two simultaneous equations for the determination of A and B, of which the solution is

$$A(\xi) = 2\beta_1(1+\beta_2^2)\gamma(\xi)\omega(\xi)/\mu R\Omega(\xi),$$
$$B(\xi) = 4\beta_1\beta_2(1+\beta_2^2)^2\gamma(\xi)\alpha(\xi)/\mu R\Omega(\xi), \tag{16}$$

where

$$\omega(\xi) = (1+\beta_2^2)^2\,\mathrm{e}^{-\xi\beta_1 d}\,\mathrm{sh}(\xi\beta_2 d) - 4\beta_1\beta_2\,\mathrm{e}^{-\xi\beta_2 d}\,\mathrm{sh}(\xi\beta_1 d),$$
$$\alpha(\xi) = \mathrm{e}^{-\xi\beta_1 d}\,\mathrm{ch}(\xi\beta_2 d) - \mathrm{e}^{-\xi\beta_2 d}\,\mathrm{ch}(\xi\beta_1 d), \tag{17}$$
$$\Omega(\xi) = (1+\beta_2^2)^2\,\mathrm{ch}(\xi\beta_1 d)\,\mathrm{sh}(\xi\beta_2 d) - 4\beta_1\beta_2\,\mathrm{sh}(\xi\beta_1 d)\,\mathrm{ch}(\xi\beta_2 d).$$

The normal stress and displacement boundary conditions for $y = 0$ lead to the following dual integral equations:

$$\int_0^\infty r^{-1}\psi(r)[1-k(r)]\cos(r\rho)\,\mathrm{d}r = g(\rho), \qquad 0 < \rho < 1,$$
$$\int_0^\infty \psi(r)\cos(r\rho)\,\mathrm{d}r = 0, \qquad \rho > 1, \tag{18}$$

where

$$\rho = x/l, \qquad \eta = y/l, \qquad r = \xi l, \qquad \psi(r) = \frac{2\beta_1(1-\beta_2^2)\gamma(r/l)}{\pi\mu R l},$$
$$h = d/l, \qquad k(r) = \omega(r/l)/\Omega(r/l), \qquad g(\rho) = w(\rho l)/l. \tag{19}$$

This set of equations is reduced to a single integral equation by selecting a functional form for $\psi(r)$ that automatically satisfies the second equation [22]. Such a form is

$$\psi(r) = \int_0^1 f(t)J_0(rt)\,\mathrm{d}t. \tag{20}$$

The first integral equation reduces to an Abel integral equation which may be inverted to give

$$f(\rho) = -\frac{2}{\pi}\frac{\mathrm{d}}{\mathrm{d}\rho}\int_0^\rho tg'(t)(\rho^2-t^2)^{-\frac{1}{2}}\,\mathrm{d}t + \int_0^1 f(r)K(r,\rho)\,\mathrm{d}r, \qquad 0<\rho<1, \tag{21}$$

where

$$K(r,\rho) = \rho\int_0^\infty \xi k(\xi)J_0(\xi r)J_0(\xi\rho)\,\mathrm{d}\xi.$$

This is a Fredholm integral equation of the second kind since its kernel is of the Hilbert–Schmidt type [23].

If a parabolic punch is considered, the function $g(\rho)$ is given by

$$g(\rho) = \frac{l\rho^2}{2r} + a, \qquad 0 \le \rho \le 1, \tag{22}$$

where a is constant and r is the radius of curvature for the punch. Defining

$$f(\rho) = \frac{l}{r}F_2(\rho) = \alpha F_2(\rho), \tag{23}$$

the integral equation becomes

$$F_2(\rho) = -\rho + \rho\int_0^1 F_2(\rho)\int_0^\infty \xi k(\xi)J_0(\xi r)J_0(\xi\rho)\,\mathrm{d}\xi\,\mathrm{d}r. \tag{24}$$

Numerical solution of this integral equation is postponed until later in the paper, but the expressions for the stresses and displacements are listed here for completeness. The stresses are

$$\begin{aligned}
\frac{\beta_1(1-\beta_2^2)}{\mu\alpha}\sigma_x(\rho,\eta) &= \int_0^1 F_2(t)[A_2\varkappa_1(\eta,\rho,\beta_1,t) - A_1\varkappa_1(\eta,\rho,\beta_2,t)]\,\mathrm{d}t \\
&\quad + \int_0^1 F_2(t)\int_0^\infty [A_1G_2(\xi,\eta) - A_2G_1(\xi,\eta)]J_0(\xi t)\cos(\xi\rho)\,\mathrm{d}\xi\,\mathrm{d}t, \\
\frac{\beta_1(1-\beta_2^2)}{\mu\alpha}\sigma_y(\rho,\eta) &= \int_0^1 F_2(t)[A_1\varkappa_1(\eta,\rho,\beta_2,t) - A_3\varkappa_1(\eta,\rho,\beta_1,t)]\,\mathrm{d}t \\
&\quad + \int_0^1 F_2(t)\int_0^\infty [A_3G_1(\xi,\eta) - A_1G_2(\xi,\eta)]J_0(\xi t)\cos(\xi\rho)\,\mathrm{d}\xi\,\mathrm{d}t, \\
\frac{(1-\beta_2^2)}{2\mu\alpha(1+\beta_2^2)}\tau_{xy}(\rho,\eta) &= \int_0^1 F_2(t)[\varkappa_2(\eta,\rho,\beta_1,t) - \varkappa_2(\eta,\rho,\beta_2,t)]\,\mathrm{d}t \\
&\quad + \int_0^1 F_2(t)\int_0^\infty [G_4(\xi,\eta) - G_3(\xi,\eta)]J_0(\xi t)\sin(\xi\rho)\,\mathrm{d}\xi\,\mathrm{d}t.
\end{aligned} \tag{25}$$

The displacements are

$$\frac{\beta_1(1-\beta_2^2)}{\alpha}u(\rho,\eta) = \int_0^1 F_2(t)\int_0^\infty [G_5(\xi,\eta)-A_{10}G_1(\xi,\eta)+A_9G_2(\xi,\eta)] \times \xi^{-1}J_0(\xi t)\sin(\xi\rho)\,\mathrm{d}\xi\,\mathrm{d}t,$$
$$\frac{(1-\beta_2^2)}{\alpha}v(\rho,\eta) = \int_0^1 F_2(t)\int_0^\infty [G_6(\xi,\eta)-A_7G_4(\xi,\eta)+A_8G_3(\xi,\eta)] \times \xi^{-1}J_0(\xi t)\cos(\xi\rho)\,\mathrm{d}\xi\,\mathrm{d}t \tag{26}$$

where

$$\begin{aligned}
&A_1 = 4\beta_1\beta_2, \quad A_2 = (1+\beta_2^2)(1+2\beta_1^2-\beta_2^2), \quad A_3 = (1+\beta_2^2)^2,\\
&A_7 = 2, \quad A_8 = (1+\beta_2^2), \quad A_9 = 2\beta_1\beta_2, \quad A_{10} = (1+\beta_2^2),\\
&G_1(\xi,\eta) = [A_1\alpha(\xi)\,\mathrm{ch}(\xi\beta_1\eta)+\omega(\xi)\,\mathrm{sh}(\xi\beta_1\eta)]/\Omega(\xi),\\
&G_2(\xi,\eta) = [A_3\alpha(\xi)\,\mathrm{ch}(\xi\beta_2\eta)+\omega(\xi)\,\mathrm{sh}(\xi\beta_2\eta)]/\Omega(\xi),\\
&G_3(\xi,\eta) = [A_1\alpha(\xi)\,\mathrm{sh}(\xi\beta_1\eta)+\omega(\xi)\,\mathrm{ch}(\xi\beta_1\eta)]/\Omega(\xi),\\
&G_4(\xi,\eta) = [A_3\alpha(\xi)\,\mathrm{sh}(\xi\beta_2\eta)+\omega(\xi)\,\mathrm{ch}(\xi\beta_2\eta)]/\Omega(\xi),\\
&G_5(\xi,\eta) = A_{10}\,\mathrm{e}^{\xi\beta_1\eta}-A_9\,\mathrm{e}^{\xi\beta_2\eta}, \quad G_6(\xi,\eta) = A_7\,\mathrm{e}^{\xi\beta_2\eta}-A_8\,\mathrm{e}^{\xi\beta_1\eta},\\
&\alpha(\xi) = \mathrm{e}^{-\xi\beta_1 h}\,\mathrm{ch}(\xi\beta_2 h)-\mathrm{e}^{-\xi\beta_2 h}\,\mathrm{ch}(\xi\beta_1 h),
\end{aligned} \tag{27}$$

and

$$\varkappa_1(\eta,\rho,\beta,t) = \frac{X}{X^2+Y^2}, \qquad \varkappa_2(\eta,\rho,\beta,t) = \left(\frac{Y}{X^2+Y^2}\right)\mathrm{sgn}(\rho), \tag{28}$$

where

$$\begin{aligned}
\sqrt{2}(X) &= \left[\sqrt{(t^2+\eta^2\beta^2-\rho^2)^2+4\eta^2\beta^2\rho^2}+t^2+\eta^2\beta^2-\rho^2\right]^{\frac{1}{2}},\\
\sqrt{2}(Y) &= \left[\sqrt{(t^2+\eta^2\beta^2-\rho^2)^2+4\eta^2\beta^2\rho^2}-t^2-\eta^2\beta^2+\rho^2\right]^{\frac{1}{2}},
\end{aligned} \tag{29}$$

for $\eta < 0$, $t > 0$, $\beta > 0$.

Since the displacements (26) are finite for the layer, a relative approach term can be established. This constant, which was lost by differentiation, can be recovered by direct evaluation of v at a point, say $\rho = \eta = 0$. The vertical displacement under the parabolic punch is from the first equation (18):

$$v(0,0) = a = \int_0^\infty r^{-1}\psi(r)[1-k(r)]\,\mathrm{d}r. \tag{30}$$

Using (20) and (23) and by assuming (see equation (63))

$$F_2(\rho) = \varkappa_1\rho+\varkappa_3\rho^3+\varkappa_5\rho^5, \tag{31}$$

the relative approach becomes

$$a/\alpha = \int_0^\infty \xi^{-1}[1-k(\xi/h)](\varkappa_1+\varkappa_3+\varkappa_5)(h/\xi)J_1(\xi/h) \\ -(2\varkappa_3+4\varkappa_5)(h/\xi)^2 J_2(\xi/h)+8\varkappa_5(h/\xi)^3 J_3(\xi/h)]\,\mathrm{d}\xi, \tag{32}$$

which can be evaluated.

The total resultant load under the punch may also be found by integrating the normal stress over the surface and then substituting the polynomial for F_2. The resultant load is

$$\frac{P}{\mu\alpha l} = \frac{\pi R}{\beta_1(\beta_2^2-1)}\int_0^1 F_2(t)\,\mathrm{d}t. \tag{33}$$

After substituting (31) into (33) and integrating, the result is

$$\frac{P}{\mu\alpha l} = \frac{\pi R}{2\beta_1(\beta_2^2-1)}(\varkappa_1+\varkappa_3/2+\varkappa_5/3). \tag{34}$$

A nondimensional effective stiffness may be defined to provide a measure of the response of the layer as

$$K = (P/\mu\alpha l)/(a/\alpha) = P/\mu a l. \tag{35}$$

Numerical values for K are included later.

To obtain the static results, the limit as the velocity approaches zero is taken. This leads to results which are contained in [24].

Antisymmetric case

If the deformation is assumed to be antisymmetric about the y axis (symmetry is still assumed about the plane $y = -d$), the appropriate transforms are

$$\bar{\Phi}(\xi, y) = \int_0^\infty \Phi(x, y)\sin(\xi x)\,\mathrm{d}x, \qquad \bar{\Psi}(\xi, y) = \int_0^\infty \Psi(x, y)\cos(\xi x)\,\mathrm{d}x. \tag{36}$$

The integral equations are the same as for the symmetric case with $\cos(\xi\rho)$ replaced by $\sin(\xi\rho)$. By choosing

$$\psi(\xi) = \xi\int_0^1 f(t)J_0(\xi t)\,\mathrm{d}t, \tag{37}$$

they reduce to

$$f(\rho) = \frac{2}{\pi}\frac{\mathrm{d}}{\mathrm{d}\rho}\int_0^\rho \frac{\mathrm{tg}(t)}{(\rho^2-t^2)^{\frac{1}{2}}}\,\mathrm{d}t + \rho\int_0^1 f(r)\int_0^\infty \xi J_0(\xi r)J_0(\xi\rho)k(\xi)\,\mathrm{d}\xi\,\mathrm{d}r. \tag{38}$$

The profile of the punch is assumed to be that of a wedge, or

$$g(\rho) = a\rho/l = \alpha\rho/2, \qquad |\rho| \le 1, \tag{39}$$

where $\alpha/2$ is the angle of inclination of the punch profile, and the integral equation becomes

$$F_2(\rho) = -\rho+\rho\int_0^1 F_2(\rho)\int_0^\infty \xi k(\xi)J_0(\xi r)J_0(\xi\rho)\,\mathrm{d}\xi\,\mathrm{d}r, \tag{40}$$

where $F_2(\rho) = -f(\rho)/\alpha$. This equation is identical to (24), indicating that the antisymmetric and the symmetric problems are reduced to the solution of the same integral equation. However, the displacements and stresses are, of course, not the same. The antisymmetric case contains stress singularities at $\rho = \pm 1$, being equal and of opposite signs. Using the expression

$$\sigma_y(\rho, 0)\frac{\beta_1(1-\beta_2^2)}{\mu R\alpha} = \int_0^1 F_2(t)\int_0^\infty \xi J_0(\xi t)\sin(\xi\rho)\,\mathrm{d}\xi\,\mathrm{d}t, \qquad |\rho| \le 1 \tag{41}$$

for the normal stress under the punch, the singularities can be isolated and the expression becomes

$$\sigma_y(\rho, 0)\frac{\beta_1(1-\beta_2^2)}{\mu R\alpha} = \frac{\rho F_2(1)}{(1-\rho^2)^{\frac{1}{2}}} + \frac{\mathrm{d}}{\mathrm{d}\rho}\int_\rho^1 (t^2-\rho^2)^{\frac{1}{2}} q'(t)\,\mathrm{d}t, \tag{42}$$

where $tq(t) = F_2(t)$ and $|\rho| \le 1$.

Since R is negative, the stress is tensile for $\rho = 1$ and compressive for $\rho = -1$. To cancel the tensile stress singularity and provide a determinate result, the solution for a flat punch is superposed in such a way as to have zero normal stress at $\rho = 1$, which is the leading edge of the punch. For a flat punch the deflection is constant and the dual integral equations are reduced by considering

$$\psi(\xi) = AJ_0(\xi) - \int_0^1 f(t)J_0(\xi t)\,\mathrm{d}t, \tag{43}$$

which satisfies the second equation automatically. The first integral equation reduces to

$$f(\rho) = -A\rho\int_0^\infty \xi J_0(\xi\rho)J_0(\xi)k(\xi)\,\mathrm{d}\xi + \rho\int_0^1 f(r)\int_0^\infty \xi J_0(\xi\rho)J_0(\xi r)k(\xi)\,\mathrm{d}\xi\,\mathrm{d}r, \qquad 0 < \rho < 1. \tag{44}$$

To determine the constant A, the normal stress for $y = 0$ is calculated and the requirement that the singularities cancel at $\rho = 1$ leads to

$$A = \alpha F_2(1). \tag{45}$$

The integral equation (44) can now be solved using this relation for A.

Superposition of the two problems leads to the following expressions for the stresses and displacements:

$$\begin{aligned}\frac{\beta_1(1-\beta_2^2)}{\mu\alpha}\sigma_x(\rho, \eta) &= F_2(1)[A_2\varkappa_1(\eta, \rho, \beta_1, 1) - A_1\varkappa_1(\eta, \rho, \beta_2, 1)] \\ &\quad - \int_0^1 \{A_2[F_1(t)\varkappa_1(\eta, \rho, \beta_1, t) + F_2(t)\chi_1(\eta, \rho, \beta_1, t)] \\ &\quad - A_1[F_1(t)\varkappa_1(\eta, \rho, \beta_2, t) + F_2(t)\chi_1(\eta, \rho, \beta_2, t)]\}\,\mathrm{d}t \\ &\quad + F_2(1)\int_0^\infty [A_1G_2(\xi, \eta) - A_2G_1(\xi, \eta)]J_0(\xi)\cos(\xi\rho)\,\mathrm{d}\xi \\ &\quad + \int_0^1\int_0^\infty [A_2G_1(\xi, \eta) - A_1G_2(\xi, \eta)][F_1(t)\cos(\xi\rho) + F_2(t)\xi\sin(\xi\rho)] \\ &\quad \times J_0(\xi t)\,\mathrm{d}\xi\,\mathrm{d}t,\end{aligned} \tag{46}$$

$$\frac{\beta_1(1-\beta_2^2)}{\mu\alpha}\sigma_y(\rho,\eta) = F_2(1)[A_1\varkappa_1(\eta,\rho,\beta_2,1)-A_3\varkappa_1(\eta,\rho,\beta_1,1)]$$
$$+\int_0^1 \{A_3[F_1(t)\varkappa_1(\eta,\rho,\beta_1,t)+F_2(t)\chi_1(\eta,\rho,\beta_1,t)]$$
$$-A_1[F_1(t)\varkappa_1(\eta,\rho,\beta_2,t)+F_2(t)\chi_1(\eta,\rho,\beta_2,t)]\}\,dt$$
$$+F_2(1)\int_0^\infty [A_3G_1(\xi,\eta)-A_1G_2(\xi,\eta)]J_0(\xi)\cos(\xi\rho)\,d\xi \tag{47}$$
$$+\int_0^1\int_0^\infty [A_1G_2(\xi,\eta)-A_3G_1(\xi,\eta)][F_1(t)\cos(\xi\rho)+F_2(t)\xi\sin(\xi\rho)]$$
$$\times J_0(\xi t)\,d\xi\,dt,$$

$$\frac{(1-\beta_2^2)}{2(1+\beta_2^2)\mu\alpha}\tau_{xy}(\rho,\eta) = F_2(1)[\varkappa_2(\eta,\rho,\beta_1,1)-\varkappa_2(\eta,\rho,\beta_2,1)]$$
$$+\int_0^1 \{F_1(t)[\varkappa_2(\eta,\rho,\beta_2,t)-\varkappa_2(\eta,\rho,\beta_1,t)]-F_2(t)\chi_2(\eta,\rho,\beta_2,t)$$
$$-\chi_2(\eta,\rho,\beta_1,t)]\}\,dt+F_2(1)\int_0^\infty [G_4(\xi,\eta)-G_3(\xi,\eta)]J_0(\xi)\sin(\xi\rho)\,d\xi \tag{48}$$
$$+\int_0^1\int_0^\infty [G_3(\xi,\eta)-G_4(\xi,\eta)][F_1(t)\sin(\xi\rho)-F_2(t)\xi\cos(\xi\rho)]$$
$$\times J_0(\xi t)\,d\xi\,dt,$$

$$\frac{\beta_1(1-\beta_2^2)}{\alpha}u(\rho,\eta) = F_2(1)\int_0^\infty [G_5(\xi,\eta)-A_{10}G_1(\xi,\eta)+A_9G_2(\xi,\eta)]\xi^{-1}J_0(\xi)\sin(\xi\rho)\,d\xi$$
$$-\int_0^1\int_0^\infty [G_5(\xi,\eta)-A_{10}G_1(\xi,\eta)+A_9G_2(\xi,\eta)] \tag{49}$$
$$\times[F_1(t)\sin(\xi\rho)-F_2(t)\xi\cos(\xi\rho)]\xi^{-1}J_0(\xi t)\,d\xi\,dt,$$

$$\frac{(1-\beta_2^2)}{\alpha}v(\rho,\eta) = F_2(1)\int_0^\infty [G_6(\xi,\eta)-A_7G_4(\xi,\eta)+A_8G_3(\xi,\eta)]$$
$$\times\xi^{-1}J_0(\xi)\cos(\xi\rho)\,d\xi-\int_0^1\int_0^\infty [G_6(\xi,\eta)-A_7G_4(\xi,\eta)+A_8G_3(\xi,\eta)] \tag{50}$$
$$\times[F_1(t)\cos(\xi\rho)+F_2(t)\xi\sin(\xi\rho)]\xi^{-1}J_0(\xi t)\,d\xi\,dt,$$

where

$$\chi_1(\eta,\rho,\beta,t) = \left[\frac{-|\rho|(X^3-3XY^2)-\eta\beta(3X^2Y-Y^3)}{(X^3-3XY^2)^2+(3X^2Y-Y^3)^2}\right]\operatorname{sgn}(\rho),$$
$$\chi_2(\eta,\rho,\beta,t) = \frac{-\eta\beta(X^3-3XY^2)+|\rho|(3X^2Y-Y^3)}{(X^3-3XY^2)^2+(3X^2Y-Y^3)^2}, \tag{51}$$

for $\eta<0$, $t>0$, $\beta>0$.

The relative approach for the wedge problem is found by considering the normal displacement for $\rho = \eta = 0$, which is

$$v(0, 0) = w. \tag{52}$$

Introducing (see equation (67))

$$F_1(\rho) = C_1\rho + C_3\rho^3 + C_5\rho^5, \tag{53}$$

the relative approach becomes

$$\begin{aligned} w/\alpha l = \int_0^\infty \xi^{-1}[1-k(\xi)][F_2(1)J_0(\xi/h) + (C_1 + C_3 + C_5)(h/\xi)J_1(\xi/h) \\ -(2C_3 + 4C_5)(h/\xi)^2 J_2(\xi/h) + 8C_5(h/\xi)^3 J_3(\xi/h)]\,\mathrm{d}\xi. \end{aligned} \tag{54}$$

The resultant normal load is given by

$$\frac{P}{\mu\alpha l} = \frac{\pi R}{\beta_1(\beta_2^2 - 1)}\left[F_2(1) - \int_0^1 F_1(t)\,\mathrm{d}t\right], \tag{55}$$

which becomes

$$\frac{P}{\mu\alpha l} = \frac{\pi R}{2\beta_1(1-\beta_2^2)}[C_1 + C_3/2 + C_5/3 - 2F_2(1)], \tag{56}$$

and the dimensionless ratio is

$$K = \left(\frac{P}{\mu\alpha l}\right)\left(\frac{\alpha l}{w}\right) = \frac{P}{\mu w}. \tag{57}$$

For the wedge problem a moment resultant may be calculated by using

$$M = \int_{-l}^{l} x\sigma_y(x, 0)\,\mathrm{d}x. \tag{58}$$

This expression leads to

$$\frac{M}{\mu\alpha l^2} = \frac{\pi R}{2\beta_1(1-\beta_2^2)}\left(\varkappa_1 + \frac{\varkappa_3}{2} + \frac{\varkappa_5}{3}\right), \tag{59}$$

and if $\delta = a/l = \alpha/2$ is the angle of the wedge

$$K_M = \frac{M}{2\mu\delta^2 l^2} = \frac{\pi R}{\alpha\beta_1(1-\beta_2^2)}\left(\varkappa_1 + \frac{\varkappa_3}{2} + \frac{\varkappa_5}{3}\right). \tag{60}$$

NUMERICAL RESULTS

Solution of Fredholm integral equation

In order to obtain numerical values for the displacements and stresses the governing integral equations must be solved. Consider first the problem of parabolic punches moving across an unstressed layer and rewrite equation (24) as

$$\theta(\rho) + h(\rho) = \int_0^1 \theta(r)K(\rho, r)\,\mathrm{d}r, \qquad 0 < \rho < 1, \tag{61}$$

where

$$\theta(\rho) = F_2(\rho) + \rho, \qquad h(\rho) = \int_0^1 rK(\rho, r)\,dr,$$

and

$$K(\rho, r) = \rho \int_0^\infty \xi k(\xi) J_0(\xi r) J_0(\xi\rho)\,d\xi.$$

This integral equation may be solved either asymptotically by expanding in powers of $1/h$ for $h = d/l \gg 1$ or numerically by representing the integral equation as a finite set of simultaneous algebraic equations in the form

$$\theta(\rho_i) + h(\rho_i) = \sum_{k=1}^{N} (\rho_k - \rho_{k-1}) K(\rho_i, r_k)\theta(r_k), \qquad i = 1, 2, \ldots, N. \tag{62}$$

The set of N equations can be solved and the function $\theta(\rho)$ determined at discrete points. In this case it is possible to represent $F_2(\rho)$ as a polynomial of the form

$$F_2(\rho) = \varkappa_1\rho + \varkappa_3\rho^3 + \varkappa_5\rho^5. \tag{63}$$

Table 1 contains values for the coefficients of $F_2(\rho)$ for various choices of c/c_2 and h. A value of 0·3 is chosen for Poisson's ratio. To indicate the behavior of the solution for increasing velocity, Fig. 2 is included. It is observed that for slow velocities the solution to the integral equation is essentially equal to the half-plane solution provided the layer is not too thin. However, the stresses do not exhibit this behavior and are more sensitive to the layer thickness. The stresses approach the half-plane solution for relatively thick layers, i.e. $h > 10$.

Computation of stresses

With the solution to the integral equation available, expressions for the stresses may be evaluated by numerical integration. Simpson's one-third rule is utilized to convert the integrals into summations and convergence is accomplished by using several test cases and comparing results. To increase the speed of convergence, the expressions are decomposed into a half-plane part and a layer part and the infinite integrals in the half-plane are evaluated analytically. The stresses are combined to provide the maximum shear stress and contour plots are developed so that comparisons may be made with photoelastic

TABLE 1. F_2 FOR $\nu = 0{\cdot}3$

c/c_2	h	$\varkappa_1$	$\varkappa_3$	$\varkappa_5$
0·2	1	−1·5505	2·5609E-1	−4·7679E-2
0·5	1	−1·7123	3·7258E-1	−7·3941E-2
0·8	1	−2·7587	1·2692	−2·9127E-1
0·2	4	−1·0342	1·6487E-3	−4·6713E-5
0·5	4	−1·0440	2·5704E-3	−8·2070E-5
0·8	4	−1·1043	1·1204E-2	−5·7218E-4
0·2	10	−1·0054	4·3317E-5	−3·5063E-7
0·5	10	−1·0070	6·7788E-5	−5·6223E-7
0·8	10	−1·0162	2·9057E-4	−8·6676E-7

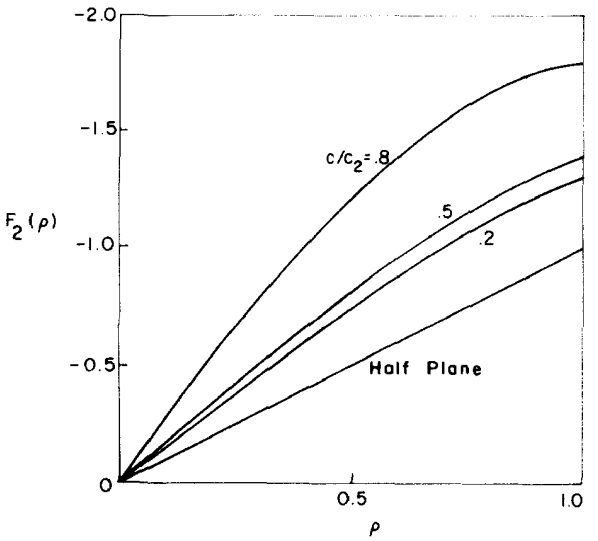

FIG. 2. Integral equation solution for parabolic punch for $h = 1$ and $c/c_2 = 0{\cdot}2, 0{\cdot}5, 0{\cdot}8$.

results. Points of maximum shear stress are easily located by examining the results and the dependence upon the velocity of the punches and thickness of the layer is readily established.

Isochromatic lines for the parabolic punch problem are shown in Fig. 3 for the half-plane and in Fig. 4 for $h = 4$. The dynamic solution appears to be very close to the static solution until the velocity ratio exceeds 0·5 and approaches the Rayleigh wave velocity, which is $0{\cdot}9274c_2$ for $\nu = 0{\cdot}3$. At this velocity a resonance phenomenon occurs and the steady velocity solution no longer exists. The authors note that for the half-plane the normal stress becomes zero, and as the velocity increases the normal stress becomes tension; it appears that no physically reasonable steady solution exists for the contact

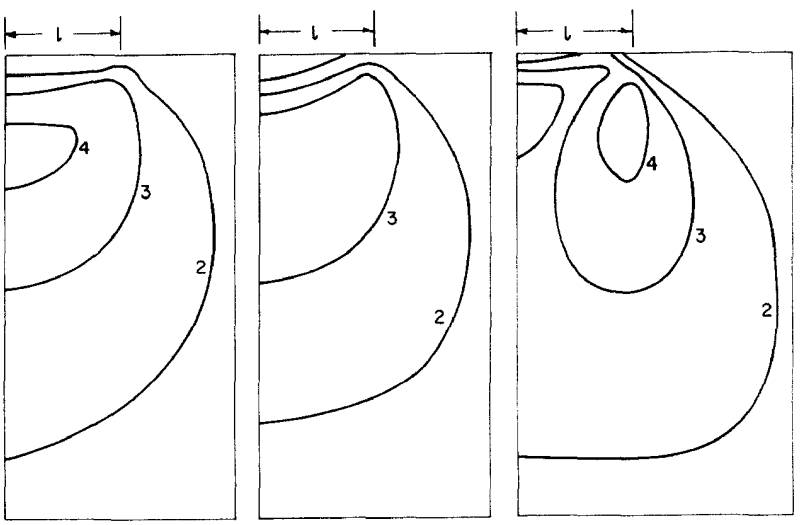

FIG. 3. Parabolic punch isochromatics ($10\tau/\mu\alpha$) for half-plane and $c/c_2 = 0{\cdot}2, 0{\cdot}5, 0{\cdot}8$.

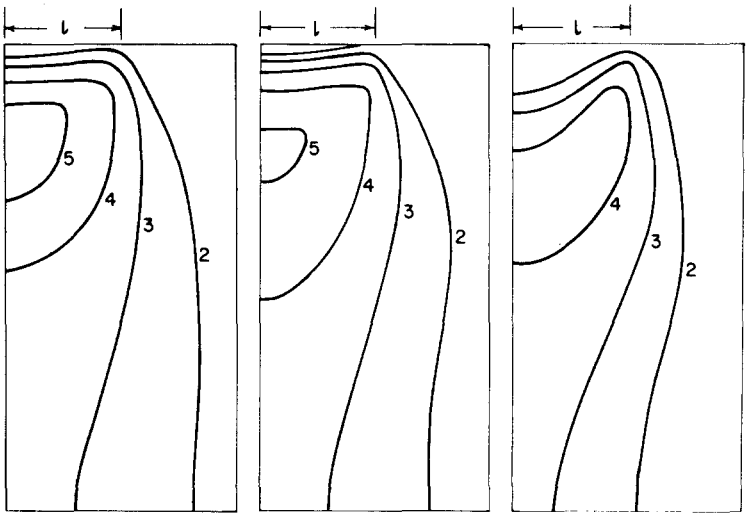

FIG. 4. Parabolic punch isochromatics ($10\tau/\mu\alpha$) for $h = 4$ and $c/c_2 = 0{\cdot}2, 0{\cdot}5, 0{\cdot}8$.

problem for $c_s \leq c \leq c_2$, where c_s is the Rayleigh wave speed [25], [26]. For velocities greater than that of shear waves, one or both of the governing equations becomes hyperbolic and the nature of the solution changes.

Wedge problem

The wedge problem is composed of two; they are an antisymmetric and a flat punch solution suitably superposed to give zero stress at the leading edge, $\rho = 1$. This scheme leads to integral equations (40) and (44) which may be rewritten as

$$F_1(\rho)+h_1(\rho) = \int_0^1 F_1(r)K(\rho, r)\,dr, \qquad 0 < \rho < 1, \tag{64}$$

$$\theta(\rho)+h_2(\rho) = \int_0^1 \theta(r)K(\rho, r)\,dr, \qquad 0 < \rho < 1, \tag{65}$$

where

$$h_1(\rho) = F_2(1)K(\rho, r), \qquad h_2(\rho) = \int_0^1 rK(\rho, r)\,dr,$$
$$K(\rho, r) = \rho\int_0^\infty \xi k(\xi)J_0(\xi r)J_0(\xi\rho)\,d\xi, \quad \text{and} \quad \theta(\rho) = F_2(\rho)+\rho. \tag{66}$$

The solution $F_2(\rho)$ is available in Table 1, and the integral equation for F_1 is solved in the same manner with results in Table 2, where

$$F_1(\rho) = C_1\rho+C_3\rho^3+C_5\rho^5, \qquad 0 < \rho < 1. \tag{67}$$

Proceeding as in the previous case, the expressions for the stresses are decomposed into half-plane and layer portions to increase convergence and are then evaluated numerically. As before, the infinite half-plane integrals can be found in closed form leaving only

TABLE 2. F_1 FOR $\nu = 0{\cdot}3$

c/c_2	h	C_1	C_3	C_5
0·2	1	2·0133	−1·3227	3·5891E-1
0·5	1	2·8839	−2·1966	6·5521E-1
0·8	1	10·820	−12·40	4·7461
0·2	4	7·2280E-2	−3·6025E-3	1·0421E-4
0·5	4	9·4364E-2	−5·7344E-3	1·9454E-4
0·8	4	2·4109E-1	−2·7265E-2	1·4545E-3
0·2	10	1·0960E-2	−8·7597E-5	4·1958E-7
0·5	10	1·4103E-2	−1·3753E-4	7·7632E-7
0·8	10	3·3167E-2	−6·0450E-4	5·4527E-6

the rapidly convergent layer integrals for numerical evaluation. Figures 5 and 6 illustrate the isochromatics for $h = 4$. The results are asymmetric about the y axis due to the superposition of the two cases. A singular stress exists at $\rho = -1$, which is the trailing edge of the punch so the fringes become dense as this point is approached.

To include the effects of prestress the equations from the Appendix are used. The determination of v_1 and v_2 is accomplished by solving a quadratic equation (75) for given isotropic material properties, prestress, and punch velocity. The solutions to the integral equations for the two cases may be developed with the roots of the quadratic now available. The weighting function $k(\xi) = \omega(\xi)/\Omega(\xi)$ has to be redefined using (81). To indicate the effect of prestress on the integral equation solution $F_2(\rho)$, Fig. 7 is included for $c/c_2 = 0{\cdot}8$ and $h = 1$. The solution for the integral equation approaches the half-plane solution for increasing prestress.

Isochromatics for the prestressed cases may be developed using the solutions to the integral equations and numerical integration of the expressions derived in the Appendix. Figure 8 indicates the behavior of the isochromatics for $h = 4$, $P/\mu = 0{\cdot}4$, and $\alpha = 0{\cdot}1$. Comparing these curves with the unstressed case shows that prestress alters the results in several ways. The values of the fringes are increased since a uniform stress is added to σ_x.

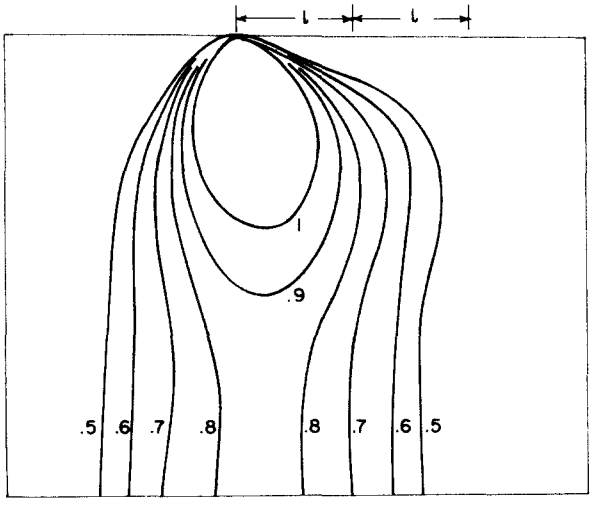

FIG. 5. Wedge punch isochromatics ($\tau/\mu\alpha$) for $h = 4$ and $c/c_2 = 0{\cdot}5$.

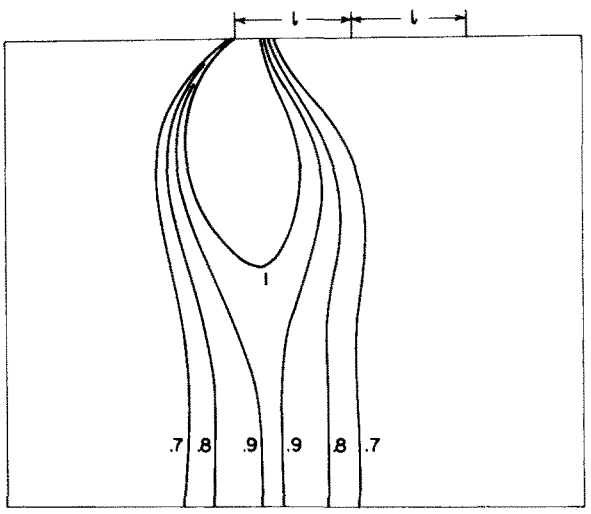

FIG. 6. Wedge punch isochromatics ($\tau/\mu\alpha$) for $h = 4$ and $c/c_2 = 0{\cdot}8$.

The other terms in the equations tend to change the shape of the curves, but one of the major effects of prestress is to increase the Rayleigh wave speed. This means that the velocity at which resonance occurs must be increased. Buckens [20] has discussed this problem.

Expressions were developed to obtain the relative approach term for the unstressed case, and thereby the solution is complete. Curves are computed for K to illustrate the response for various values of layer thickness and punch velocity. Figure 9 gives results for the parabolic punch problem for $\nu = 0{\cdot}3$ and no prestress. Increasing the layer thickness or punch velocity decreases the stiffness of the layer. For a half-plane or a punch moving at the velocity of Rayleigh waves, $K = 0$, which means the effective resistance to the load has disappeared.

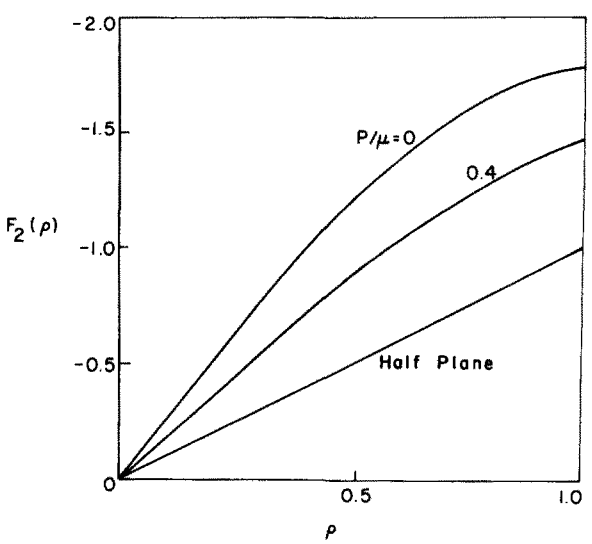

FIG. 7. Integral equation solution for parabolic punch for $h = 1$, $c/c_2 = 0{\cdot}8$ and $P/\mu = 0{\cdot}0, 0{\cdot}4$.

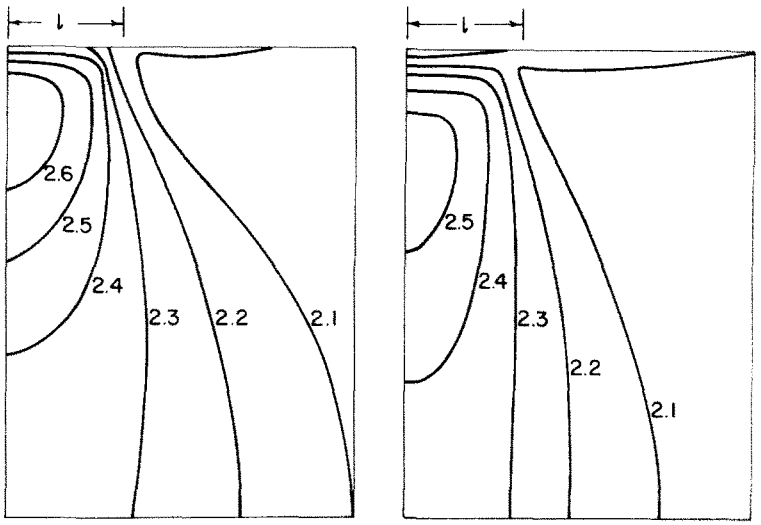

FIG. 8. Parabolic punch isochromatics ($10\tau/\mu$) for $h = 4$, $P/\mu = 0{\cdot}4$, $\alpha = 0{\cdot}1$, and $c/c_2 = 0{\cdot}2, 0{\cdot}8$.

To obtain a qualitative verification of the results a photoelastic experiment was conducted for the static case. Isochromatics were obtained and are shown in Figs. 10 and 11 for the case of parabolic punches indenting a layer which was unstressed in the first case and prestressed with $\sigma_x/\mu\alpha = 0{\cdot}552$ in the second case. The same isochromatics were computed using the theoretical expressions for $\nu = 0{\cdot}465$, $\mu = 151$ psi, $h = 7{\cdot}5$, and $\alpha = \frac{1}{13}$,

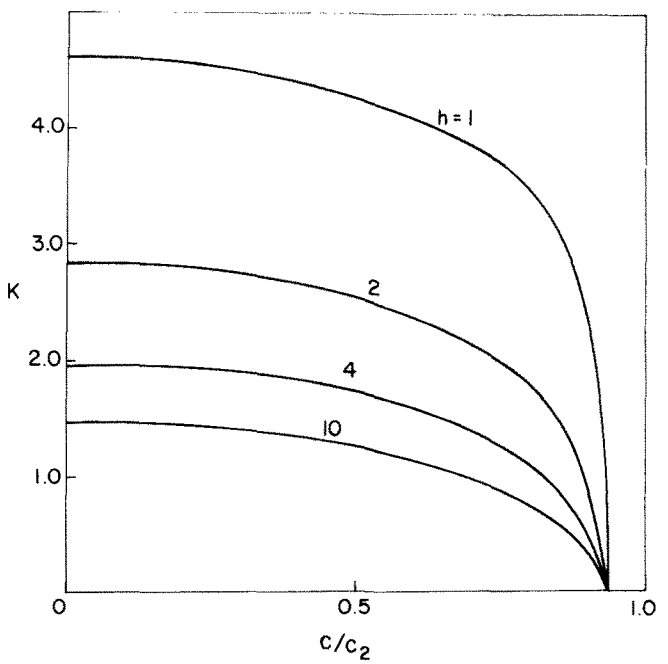

FIG. 9. Effective stiffness vs. velocity for parabolic punch case.

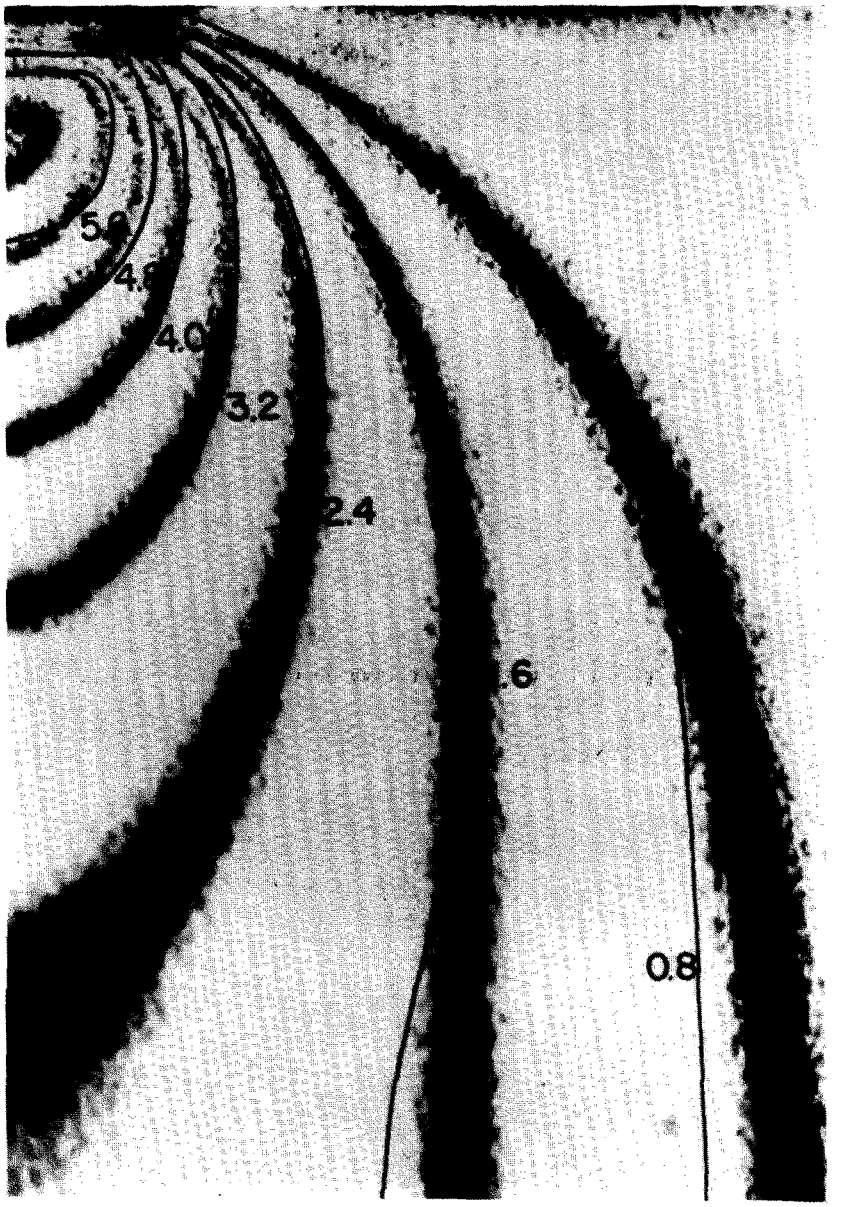

FIG. 10. Theoretical and experimental results for parabolic punch isochromatics.

facing p. 810

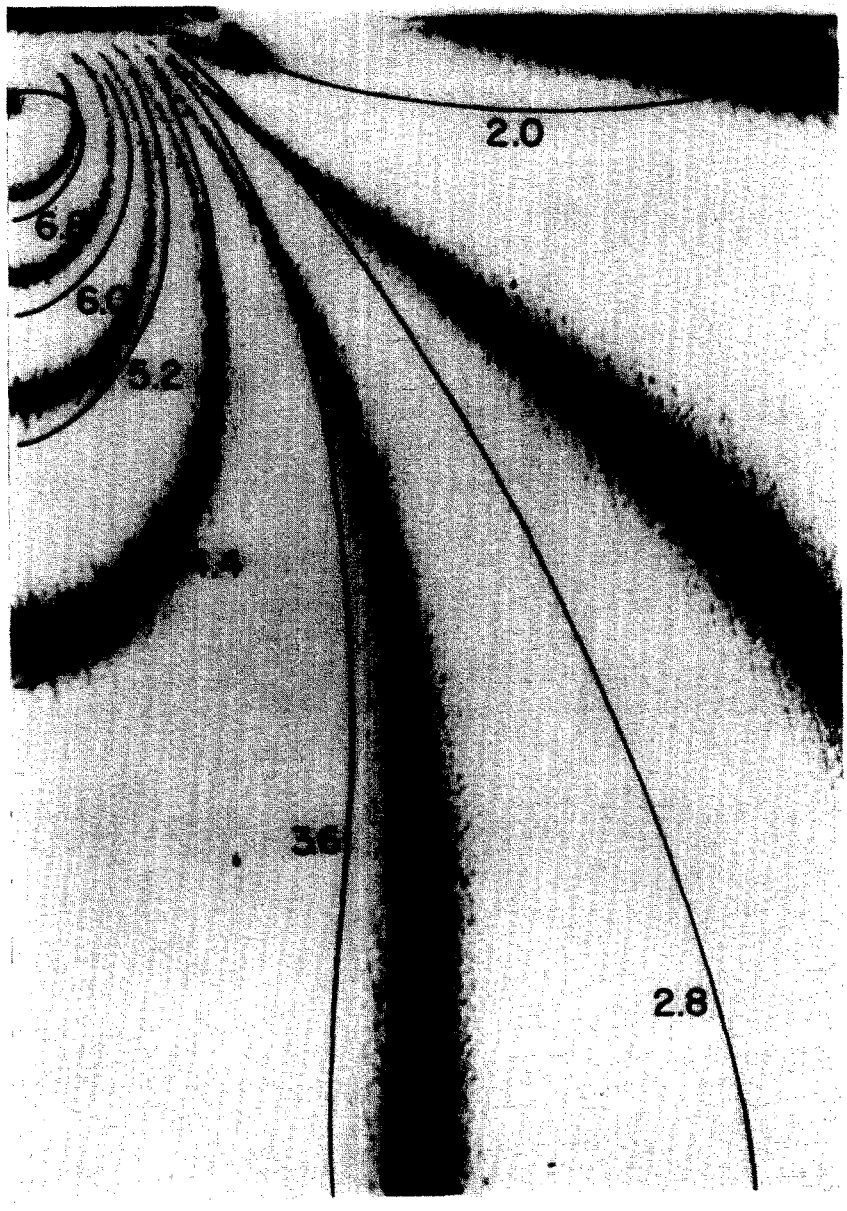

FIG. 11. Theoretical and experimental results for parabolic punch isochromatics including prestress.

and have been superposed on the figures to indicate the degree of agreement. The half-plane results were also computed for this case and it was found that the layer solution increased the fringe order by approximately one. Near the center of the layer ($y = -d$), however, the fringe pattern, as well as the order, was altered as can be seen in Figs. 3 and 4 for a similar case. Additional computations were made for various values of h and it was concluded that for $h > 10$, the stress distribution could be adequately predicted with a half-plane solution.

SUMMARY

Several problems appropriate to the geometry of a layer have been studied. For indentation problems, dual integral equations arise which may be solved by analytical, numerical or asymptotic methods, depending upon the final results desired and the relative difficulty involved. The examples studied utilize a numerical method for the solution of the integral equation since the final results were to be the isochromatics in the interior of the layer. The expressions for these stresses contain integrals that had to be computed numerically so an asymptotic scheme would not be especially helpful.

Examination of the figures indicates that the solution is approximately given by the static solution until $c > 0{\cdot}5c_2$. The thickness of the layer influences the solution to the integral equations, e.g. when $d < 4l$, otherwise the half-plane solution is sufficient, approximately. However, the stress distribution within the layer is more sensitive to the layer thickness since the half-plane solution is approximately valid only when $d > 10l$. The response in a global sense may be obtained from Fig. 9. The curves are flat for $c < 0{\cdot}5c_2$ but are rapidly changing in the region $0{\cdot}5c_2 < c < c_s$ as the resonance point is approached. Also, as the layer thickness decreases, K increases and in the limit becomes infinite.

The authors note that in a recent paper, Wang, [27] has solved similar dual integral equations that possess a different weight function. In his solution method the dual integral equations are reduced to a Fredholm integral equation of the first kind, rather than of the second kind as in the present development.

Acknowledgments—This research was supported in part by the U.S. Air Force under Grant No. AF-AFOSR-100-67 monitored by the Air Force Office of Scientific Research. Financial assistance in the form of the Royal E. Cabell Fellowship from Northwestern University is acknowledged. The authors are also grateful to the Northwestern University Vogelback Computing Center and the National Science Foundation whose fund helped in the establishment of the Center.

REFERENCES

[1] ELIZABETH YOFFE, The moving griffith crack. *Phil. Mag.* **42**, 739–750 (1951).
[2] I. N. SNEDDON, The stresses produced by a pulse of pressure moving along the surface of a semi-infinite solid. *Rend. Circ. Math. Palermo*, **2**, 57 (1952).
[3] J. R. M. RADOK, On the solution of problems of dynamic plane elasticity. *Q. appl. Math.* **14**, 289–298 (1956).
[4] I. N. SNEDDON and D. S. BERRY, The classical theory of elasticity. *Handbuch der Physik*, Vol. 6, pp. 118–122. Springer (1958).
[5] J. COLE and J. HUTH, Stresses produced in a half plane by moving loads. *J. appl. Mech.* **25**, 433–436 (1958).
[6] D. D. ANG, Transient motion of a line load on the surface of an elastic half-space. *Q. appl. Math.* **18**, 251–256 (1960).
[7] R. G. PAYTON, Transient motion of an elastic half-space due to a moving surface line load. *Int. J. Engng Sci.* **5**, 49–79 (1967).
[8] L. S. D. MORLEY, Elastic plate with loads travelling at uniform velocity along the bounding surfaces. *Q. Jl Mech. appl. Math.* **15**, 193–213 (1962).

[9] G. EASON, The stresses produced in a semi-infinite solid by a moving surface force. *Int. J. Engng Sci.* **2**, 581–609 (1965).
[10] R. G. PAYTON, An application of the dynamic Betti–Rayleigh reciprocal theorem to moving-point loads in elastic media. *Q. appl. Math.* **21**, 299–313 (1964).
[11] M. A. BIOT, *Mechanics of Incremental Deformations*. Wiley (1965).
[12] A. E. GREEN and J. E. ADKINS, *Large Elastic Deformations and Non-Linear Continuum Mechanics*. Oxford University Press (1960).
[13] T. W. WRIGHT, Plate and rod vibrations with initial stress. *J. appl. Mech.* **33**, 134–140 (1966).
[14] T. W. WRIGHT, Some initial stress problems in the general theory of elasticity. Ph.D. Thesis, Cornell University, Ithaca, New York (1964).
[15] A. E. GREEN, R. S. RIVLIN and R. T. SHIELD, General theory of small elastic deformations superposed on finite elastic deformations. *Proc. R. Soc.* **A211**, 128–154 (1952).
[16] V. V. NOVOZHILOV, *Foundations of the Nonlinear Theory of Elasticity*. Graylock Press (1953). Translated from the Russian edition (1948).
[17] A. E. GREEN and W. ZERNA, *Theoretical Elasticity*. Oxford University Press (1963).
[18] W. T. CHEN, Displacement discontinuity over a transversely isotropic elastic half-space. *IBM Journal of Research and Development* **8**, 435–442 (1964).
[19] W. T. CHEN, On some problems in transversely isotropic elastic materials. *J. appl. Mech.* **33**, 347–355 (1966).
[20] F. BUCKENS, The velocity of rayleigh waves along a prestressed semi-infinite medium assuming a two-dimensional anisotropy, *Annali di Geofisica*, **11** 99–112 (1958).
[21] I. N. SNEDDON, *Fourier Transforms*. McGraw-Hill (1951).
[22] E. T. COPSON, On certain dual integral equations. *Proc. Glasg. math. Ass.* **5**, 21–24 (1961).
[23] R. COURANT and D. HILBERT, *Methods of Mathematical Physics*. Vol. 1, Interscience (1953).
[24] Y. S. UFLYAND, Survey of articles on the applications of integral transforms in the theory of elasticity. translated by W. J. A. WHYTE, edited by I. N. SNEDDON, North Carolina State University, Technical Report No. AFOSR-65-1556, pp. 24–26 (1965).
[25] J. W. CRAGGS and A. M. ROBERTS, On the motion of a heavy cylinder over the surface of an elastic solid. *J. appl. Mech.* **34**, 207–209 (1967).
[26] R. V. GOL'DSHTEIN, Rayleigh waves and resonance phenomena in elastic bodies. *J. appl. Math. Mech.* **29**, 608–619 (1965).
[27] C. F. WANG, Elastic contact of a strip pressed between two cylinders. *J. appl. Mech.* **35**, 279–284 (1968).

APPENDIX. INDENTATIONS OF A PRESTRESSED LAYER

Symmetric case

The equilibrium equations in terms of incremental stresses s_x, s_y, s_{xy}, are [11]

$$\frac{\partial s_x}{\partial x'}+\frac{\partial s_{xy}}{\partial y'}+(S_x-S_y)\frac{\partial \omega}{\partial y'}=\rho\frac{\partial^2 u}{\partial t^2},$$
$$\frac{\partial s_{xy}}{\partial x'}+\frac{\partial s_y}{\partial y'}+(S_x-S_y)\frac{\partial \omega}{\partial x'}=\rho\frac{\partial^2 v}{\partial t^2}, \tag{68}$$

where u and v are displacements in the x' and y' directions, respectively, and ω denotes the rotation,

$$2\omega=\frac{\partial v}{\partial x'}-\frac{\partial u}{\partial y'}. \tag{69}$$

The prestress terms S_x and S_y act along the x' and y' axes, respectively. Assuming the layer is prestressed only in the x' direction, $S_y=0$ and $S_x=P$. The material is chosen to be

orthotropic and the incremental displacements are assumed small leading to the linear relations

$$s_x = B_{11}e_x + B_{12}e_y = B_{11}\frac{\partial u}{\partial x'} + B_{12}\frac{\partial v}{\partial y'},$$

$$s_y = B_{21}e_x + B_{22}e_y = B_{21}\frac{\partial u}{\partial x'} + B_{22}\frac{\partial v}{\partial y'}, \tag{70}$$

$$s_{xy} = 2Qe_{xy} = Q\left(\frac{\partial v}{\partial x'} + \frac{\partial u}{\partial y'}\right).$$

The existence of a strain energy function implies the following relationship between the material constants:

$$B_{21} - B_{12} = S_x - S_y = P. \tag{71}$$

For uniform motion with velocity c along the x' axis, the steady motion transformation $x = x' - ct$, $y = y'$, $z = z'$, is used to eliminate time from the equations.

The potential $\varphi(x, y)$ is introduced [18], with the displacements defined by

$$u = \frac{\partial \varphi}{\partial x}, \qquad v = k\frac{\partial \varphi}{\partial y}, \tag{72}$$

where k is a constant. Substituting equation (72) into the governing equations leads to

$$\left[\frac{B_{11} - \rho c^2}{Q - \frac{P}{2} + k\left(B_{12} + Q + \frac{P}{2}\right)}\right]\frac{\partial^2 \varphi}{\partial x^2} + \frac{\partial^2 \varphi}{\partial y^2} = 0,$$

$$\left[\frac{\left(Q + \frac{P}{2} - \rho c^2\right)k + B_{21} + Q - \frac{P}{2}}{kB_{22}}\right]\frac{\partial^2 \varphi}{\partial x^2} + \frac{\partial^2 \varphi}{\partial y^2} = 0. \tag{73}$$

For equation (73) to have a nontrivial solution they must be identical, which gives a relation in terms of a constant v,

$$v = \frac{B_{11} - \rho c^2}{Q - \frac{P}{2} + k\left(B_{12} + Q + \frac{P}{2}\right)} = \frac{\left(Q + \frac{P}{2} - \rho c^2\right)k + B_{21} + Q - \frac{P}{2}}{kB_{22}}. \tag{74}$$

Eliminating k, equation (74) may be rewritten as

$$v^2 B_{22}\left(Q - \frac{P}{2}\right) - v\left[B_{22}(B_{11} - \rho c^2) + \left(Q + \frac{P}{2} - \rho c^2\right)\left(Q - \frac{P}{2}\right) - \left(B_{12} + Q + \frac{P}{2}\right)^2\right]$$
$$+ \left(Q + \frac{P}{2} - \rho c^2\right)(B_{11} - \rho c^2) = 0. \tag{75}$$

Equation (75) contains two roots v_1 and v_2 which are assumed to be unequal and to have positive real parts (see [18] and [19]). For each root there is a corresponding value

of k given by equation (74) and they are designated k_1 and k_2. Such a designation leads to two potential functions φ_1 and φ_2, with the displacements becoming

$$u = \frac{\partial \varphi_1}{\partial x} + \frac{\partial \varphi_2}{\partial x}, \qquad v = k_1 \frac{\partial \varphi_1}{\partial y} + k_2 \frac{\partial \varphi_2}{\partial y}. \tag{76}$$

As in the previous case, the solution for the layer is decomposed into a half-plane solution and a portion for the undamaged layer.

The boundary conditions are

$$\begin{aligned} s_y &= 0, & |x| &> l, & y &= 0, \\ s_{xy} - Pe_{xy} &= 0, & -\infty &< x < \infty, & y &= 0, \\ v &= w(x), & |x| &< l, & y &= 0, \\ s_{xy} - Pe_{xy} &= 0, & -\infty &< x < \infty, & y &= -d, \\ v &= 0, & -\infty &< x < \infty, & y &= -d. \end{aligned} \tag{77}$$

It follows that the solution has the form

$$\begin{aligned} \varphi_1(x, y) &= \varphi_{1h}(x, y) + \frac{2}{\pi} \int_0^\infty [A_1(\xi) \operatorname{ch}(\xi \sqrt{v_1} y) + B_1(\xi) \operatorname{sh}(\xi \sqrt{v_1} y)] \xi^{-2} \cos(\xi x)\, d\xi, \\ \varphi_2(x, y) &= \varphi_{2h}(x, y) + \frac{2}{\pi} \int_0^\infty [A_2(\xi) \operatorname{ch}(\xi \sqrt{v_2} y) + B_2(\xi) \operatorname{sh}(\xi \sqrt{v_2} y)] \xi^{-2} \cos(\xi x)\, d\xi. \end{aligned} \tag{78}$$

Substituting equations (78) into the stress boundary conditions for $y = 0$ leads to

$$\begin{aligned} B_1 &= \frac{B}{\sqrt{v_1}(1 + k_1)}, & B_2 &= \frac{-B}{\sqrt{v_2}(1 + k_2)}, \\ A_1 &= \frac{A}{B_{22} k_1 v_1 - B_{12} - P}, & A_2 &= \frac{-A}{B_{22} k_2 v_2 - B_{12} - P}, \end{aligned} \tag{79}$$

where A and B are

$$\begin{aligned} A(\xi) &= \sqrt{v_1 v_2}(1 + k_1)(1 + k_2)(B_{22} k_2 v_2 - B_{12} - P) \\ &\quad \times (B_{22} k_1 v_1 - B_{12} - P) \alpha(\xi) \gamma(\xi) / R\Omega(\xi), \\ B(\xi) &= \sqrt{v_1 v_2}(1 + k_1)(1 + k_2) \omega(\xi) \gamma(\xi) / R\Omega(\xi), \end{aligned} \tag{80}$$

and

$$\begin{aligned} R &= \sqrt{v_2}(1 + k_2)(B_{22} k_1 v_1 - B_{12} - P) - \sqrt{v_1}(1 + k_1)(B_{22} k_2 v_2 - B_{12} - P), \\ \alpha(\xi) &= e^{-\xi \sqrt{v_1} d} \operatorname{ch}(\xi \sqrt{v_2} d) - e^{-\xi \sqrt{v_2} d} \operatorname{ch}(\xi \sqrt{v_1} d), \\ \omega(\xi) &= \sqrt{v_2}(1 + k_2)(B_{22} k_1 v_1 - B_{12} - P) e^{-\xi \sqrt{v_1} d} \operatorname{sh}(\xi \sqrt{v_2} d) \\ &\quad - \sqrt{v_1}(1 + k_1)(B_{22} k_2 v_2 - B_{12} - P) e^{-\xi \sqrt{v_2} d} \operatorname{sh}(\xi \sqrt{v_1} d), \\ \Omega(\xi) &= \sqrt{v_2}(1 + k_2)(B_{22} k_1 v_1 - B_{12} - P) \operatorname{sh}(\xi \sqrt{v_2} d) \operatorname{ch}(\xi \sqrt{v_1} d) \\ &\quad - \sqrt{v_1}(1 + k_1)(B_{22} k_2 v_2 - B_{12} - P) \operatorname{sh}(\xi \sqrt{v_1} d) \operatorname{ch}(\xi \sqrt{v_2} d). \end{aligned} \tag{81}$$

To satisfy the displacement condition on $y = 0$ and the requirement of vanishing normal stress for $|x| > l$, dual integral equations arise which become identical to equation (24) except for $k(\xi) = \omega(\xi)/\Omega(\xi)$, which is defined as above.

This Fredholm integral equation of the second kind may be solved using numerical or iterative methods. $F_2(\rho)$ may be represented by a polynomial and the stresses may be obtained by evaluating the following expressions:

$$\begin{aligned} \sigma_x &= s_x + P, \\ \sigma_y &= s_y, \\ \tau_{xy} &= s_{xy} + P\omega, \end{aligned} \tag{82}$$

which lead to

$$\begin{aligned} \frac{\sqrt{v_1 v_2}(k_2 - k_1)}{\alpha}\sigma_x(\rho, \eta) &= \int_0^1 F_2(t)[A_2\kappa_1(\eta, \rho, \sqrt{v_1}, t) - A_4\kappa_1(\eta, \rho, \sqrt{v_2}, t]\,\mathrm{d}t \\ &\quad + \int_0^1 F_2(t)\int_0^\infty [A_4 G_2(\xi, \eta) - A_2 G_1(\xi, \eta)]J_0(\xi t) \\ &\quad \times \cos(\xi\rho)\,\mathrm{d}\xi\,\mathrm{d}t + \sqrt{v_1 v_2}(k_2 - k_1)\frac{P}{\alpha}, \\ \frac{\sqrt{v_1 v_2}(k_2 - k_1)}{\alpha}\sigma_y(\rho, \eta) &= \int_0^1 F_2(t)[A_1\varkappa_1(\eta, \rho, \sqrt{v_2}, t) - A_3\varkappa_1(\eta, \rho, \sqrt{v_1}, t)\,\mathrm{d}t \\ &\quad + \int_0^1 F_2(t)\int_0^\infty [A_3 G_1(\xi, \eta) - A_1 G_2(\xi, \eta)]J_0(\xi t)\cos(\xi\rho)\,\mathrm{d}\xi\,\mathrm{d}t, \\ \frac{(k_2 - k_1)}{\alpha}\tau_{xy}(\rho, \eta) &= \left(Q - \frac{P}{2}\right)(1 + k_1)(1 + k_2)\int_0^1 F_2(t)[\varkappa_2(\eta, \rho, \sqrt{v_1}, t) \\ &\quad - \varkappa_2(\eta, \rho, \sqrt{v_2}, t)]\,\mathrm{d}t + P\int_0^1 F_2(t)[A_8\varkappa_2(\eta, \rho\sqrt{v_1}, t) \\ &\quad - A_7\varkappa_2(\eta, \rho, \sqrt{v_2}, t)]\,\mathrm{d}t + \int_0^1 F_2(t)\int_0^\infty [A_5 G_4(\xi, \eta) \\ &\quad - A_6 G_3(\xi, \eta)]J_0(\xi t)\sin(\xi\rho)\,\mathrm{d}\xi\,\mathrm{d}t. \end{aligned} \tag{83}$$

The displacements are

$$\begin{aligned} \sqrt{v_1 v_2}(k_2 - k_1)u(\rho, \eta)/\alpha &= \int_0^1 F_2(t)\int_0^\infty [G_5(\xi, \eta) - A_{10}G_1(\xi, \eta) \\ &\quad + A_9 G_2(\xi, \eta)]\xi^{-1}J_0(\xi t)\sin(\xi\rho)\,\mathrm{d}\xi\,\mathrm{d}t, \\ (k_2 - k_1)v(\rho, \eta)/\alpha &= \int_0^1 F_2(t)\int_0^\infty [G_6(\xi, \eta) - A_7 G_4(\xi, \eta) \\ &\quad + A_8 G_3(\xi, \eta)]\xi^{-1}J_0(\xi t)\cos(\xi\rho)\,\mathrm{d}\xi\,\mathrm{d}t, \end{aligned} \tag{84}$$

where

$$
\begin{aligned}
A_1 &= \sqrt{v_1}(1+k_1)(B_{22}k_2v_2 - B_{12} - P),\\
A_2 &= \sqrt{v_2}(1+k_2)(B_{11} - B_{12}k_1v_1),\\
A_3 &= \sqrt{v_2}(1+k_2)(B_{22}k_1v_1 - B_{12} - P),\\
A_4 &= \sqrt{v_1}(1+k_1)(B_{11} - B_{12}k_2v_2),\\
A_5 &= (1+k_1)[Q+k_2(Q+P)], \qquad A_6 = (1+k_2)[Q+k_1(Q+P)],\\
A_7 &= k_2(1+k_1), \qquad A_8 = k_1(1+k_2),\\
A_9 &= \sqrt{v_1}(1+k_1), \qquad A_{10} = \sqrt{v_2}(1+k_2),
\end{aligned}
\tag{85}
$$

and the definitions for the functions G_i are given by equations (27) with β_1 and β_2 replaced by $\sqrt{v_1}$ and $\sqrt{v_2}$, respectively.

For the case of zero prestress and isotropic material properties,

$$
v_1 = \beta_1^2, \qquad v_2 = \beta_2^2, \qquad k_1 = 1, \qquad k_2 = 1/\beta_2^2,
\tag{86}
$$

which leads to

$$
\begin{gathered}
A_1 = 4\beta_1\mu, \qquad A_2 = \mu(1+\beta_2^2)(1+2\beta_1^2-\beta_2^2)/\beta_2,\\
A_3 = \mu(1+\beta_2^2)^2/\beta_2, \qquad A_4 = 4\beta_1\mu, \qquad A_5 = A_6 = 2\mu(1+\beta_2^2)/\beta_2^2.\\
A_7 = 2/\beta_2^2, \qquad A_8 = (1+\beta_2^2)/\beta_2^2,\\
A_9 = 2\beta_1, \qquad A_{10} = (1+\beta_2^2)/\beta_2.
\end{gathered}
\tag{87}
$$

The wedge punch case including prestress presents no new difficulties and is not investigated here.

(*Received* 18 *September* 1968; *revised* 19 *December* 1968)

Абстракт—Рассматривается задача слоя в плоской деформации (или напряжениях), подвергающего протяжке без трения между двумя штампами заданного профиля. Слой движется с постоянной скоростью вдоль поверхностей штампов. Сохраняется симметрия вокруя серединной поверхности слоя. Используются трансформации Фуръе для сведения задачи к решению системы парных интегралъных уравнений. Стандартной мето ддает интеградъное уравнение Фредголъма, решаемое численно для параболического и клино-образного штампов. Сравниваются статические резулътаты с фотоупругим экспериментом. Представляется кратко анализ, учитывающий эффект предварителъных напряжений.